The zebrafish *van gogh* mutation disrupts *tbx1*, which is involved in the DiGeorge deletion syndrome in humans

Tatjana Piotrowski[1,2,*,†], Dae-gwon Ahn[3,*], Thomas F. Schilling[4], Sreelaja Nair[4], Ilya Ruvinsky[5], Robert Geisler[6], Gerd-Jörg Rauch[6], Pascal Haffter[6], Leonard I. Zon[7], Yi Zhou[7], Helen Foott[7], Igor B. Dawid[1] and Robert K. Ho[3]

[1]National Institutes of Health, NICHD, LMG, Bldg. 6B, 9000 Rockville Pike, Bethesda, MD 20892, USA
[2]University of Utah, Department of Neurobiology and Anatomy, 401 MREB, Salt Lake City, UT 84132, USA
[3]University of Chicago, Department of Organismal Biology and Anatomy, Chicago, IL 60637, USA
[4]University of California, Irvine, Department of Developmental and Cell Biology, Irvine, CA 92697, USA
[5]Princeton University, Department of Molecular Biology, Princeton, NJ 08544, USA
[6]Max-Planck-Institute for Developmental Biology, Spemannstr.35, 72076, Tübingen, Germany
[7]Howard Hughes Medical Institute, Division of Hematology/Oncology, Children's Hospital, Boston, MA 02115, USA
*These authors contributed equally to this work
†Author for correspondence (e-mail: piotrowski@neuro.utah.edu)

Accepted 25 June 2003

Development 130, 5043-5052
© 2003 The Company of Biologists Ltd
doi:10.1242/dev.00704

Summary

The *van gogh* (*vgo*) mutant in zebrafish is characterized by defects in the ear, pharyngeal arches and associated structures such as the thymus. We show that *vgo* is caused by a mutation in *tbx1*, a member of the large family of T-box genes. *tbx1* has been recently suggested to be a major contributor to the cardiovascular defects in DiGeorge deletion syndrome (DGS) in humans, a syndrome in which several neural crest derivatives are affected in the pharyngeal arches. Using cell transplantation studies, we demonstrate that *vgo/tbx1* acts cell autonomously in the pharyngeal mesendoderm and influences the development of neural crest-derived cartilages secondarily. Furthermore, we provide evidence for regulatory interactions between *vgo/tbx1* and *edn1* and *hand2*, genes that are implicated in the control of pharyngeal arch development and in the etiology of DGS.

Key words: *van gogh* (*vgo*), *tbx1*, *endothelin1*, Pharyngeal arch development, DiGeorge syndrome, Endodermal pouches, Aortic arches, Zebrafish

Introduction

The development of the pharyngeal arches in vertebrates requires an intricate interplay between the pharyngeal endoderm, the mesodermal core of the arches, and neural crest cells. As yet, little is known about the molecular nature of these tissue interactions. The zebrafish mutant *van gogh* (*vgo*) is characterized by defects in the pharyngeal arches and associated structures, including fusion and loss of neural crest-derived pharyngeal cartilages, reductions in endodermal pouches and aortic arches, and the absence of the thymus (Piotrowski and Nüsslein-Volhard, 2000; Piotrowski et al., 1996). In addition, the otic vesicles in *vgo* mutants are reduced in size and some sensory patches within the mature ear are absent (Piotrowski and Nüsslein-Volhard, 2000; Whitfield et al., 1996).

The phenotype of homozygous *vgo* mutants bears striking resemblance to humans afflicted with DiGeorge syndrome (DGS). DGS is one of the most common developmental diseases in humans, affecting approximately 1 in 4000 live births (Scambler, 2000). Individuals with DGS are characterized by craniofacial defects, aortic arch malformations, thymus hypoplasia, conotruncal heart defects and hearing loss (Ryan et al., 1997). The majority of individuals carry a heterozygous deletion located on chromosomal region 22q11.2. This region comprises ~30 genes and is called the DiGeorge critical region (DGCR). Combined studies of heterozygous deletions within the DGCR and knockout experiments in mice have identified *Tbx1* as a major genetic determinant of aortic arch malformations in DGS (Jerome and Papaioannou, 2001; Lindsay et al., 2001; Merscher et al., 2001). *Tbx1* encodes a transcription factor belonging to a gene family characterized by a highly conserved DNA-binding domain called the T-box. T-box genes are important regulators of embryonic development, examples include the founding family member *T* or *Brachyury*, which, when mutated in mice or zebrafish, leads to the loss of notochord and tail structures (Kispert et al., 1995; Schulte-Merker et al., 1994). Other examples are mutations in *TBX5* and *TBX3*, which are responsible for human Holt-Oram and Ulnar-mammary syndromes, respectively, in which formation of limbs and cardiovascular system is disrupted (Bamshad et al., 1997; Basson et al., 1997), and the *spadetail* mutation in zebrafish, which affects the formation of trunk somites (Griffin et al., 1998).

We show that the zebrafish *vgo* mutant is defective in *tbx1*, which is required for interactions between the cranial mesendoderm and the neural crest cells that form the pharyngeal cartilages. Transplantation of wild-type endoderm into *vgo/tbx1* mutants induces cartilage formation, which

indicates that *tbx1* acts autonomously in the endoderm. Consequently, the neural crest defects are secondary to endodermal defects in *vgo/tbx1* mutants, as has been previously suggested (Piotrowski and Nuesslein-Volhard, 2000). The zebrafish *vgo/tbx1* mutant offers the opportunity to study pharyngeal arch development in cellular detail and may contribute further to the understanding of DGS pathogenesis.

Materials and methods

Cloning of *tbx1*

A zebrafish λgt11 cDNA library (gift from Kai Zinn) constructed from 30- to 33-hour old embryos was screened under low stringency conditions (50°C) using a mixture of ^{32}P-labeled oligonucleotide probes prepared from various mouse T-box sequences. Positive plaques were isolated and the cDNAs subcloned into pBluescript for sequencing. One clone with an open reading frame of 460 amino acids contained a T-box sequence highly similar to the *Tbx1* gene of mouse and human, and thus was named *tbx1* (GenBank Accession Number AY294284).

Sequence analysis of *tbx1* in *vgo*

Primers were designed using the sequences flanking the exon-intron boundaries of *tbx1*. Genomic DNA was extracted from a pool of 4-day-old homozygous mutant embryos. PCRs were performed separately for each exon and the resulting products were cloned into the pGEM-T-Easy (Promega) vector for sequencing. Mutations were confirmed independently by repeat PCR reactions.

Meiotic and radiation hybrid mapping

The *vgo^{tm208}* allele was generated in the Tübingen background in a large scale mutagenesis screen (Haffter et al., 1996; Piotrowski et al., 1996). To produce a polymorphic strain for genetic mapping, the fish carrying this allele was crossed to wik fish (Knapik et al., 1996; Rauch et al., 1997). Homozygous and sibling embryos were phenotypically scored at 4 dpf and fixed separately in 4% paraformaldehyde overnight. For extraction of genomic DNA individual embryos were placed in 96-well PCR plates and processed as described (Rauch et al., 1997). Bulk segregant analysis with SSLP markers was used to identify the linkage group. Analysis of SSCP markers in individual embryos was used to fine map the mutation. Radiation hybrid mapping of *tbx1* was performed as described (Hukriede et al., 1999), using forward primer 5′-AACATGTACTCTGCGACGAGTGCAC-3′ and reverse primer 5′-CACGGATCTGCTAAAGGTGGTCTAG-3′ on the LN54 panel. The PCR conditions were 95°C for 4 minutes, 35 cycles of 94°C for 30 seconds, 65°C for 30 seconds, 72°C for 30 seconds each, followed by 72°C for 7 minutes. The results were analyzed by interactive mapping software available at http://www.mgchd1.nichd.nih.gov:8000/zfrh/beta.cgi

Linkage analysis between *tbx1* and *vgo^{tm208}*

The A to T transition mutation in the *vgo^{tm208}* allele leads to the loss of an *Alw*N1 restriction site in the *tbx1* gene, which co-segregated with the mutation. Genomic DNA was amplified by PCR using the forward 5′-GCTCTGGAGTGAACTTGATTACCTG-3′ and reverse 5′-AACGGTCAAGTAGGCCTGTAGCTAC-3′ primers that flank the mutation. The PCR product was digested with *Alw*N1 and analyzed on a 3% MetaPhor agarose gel (BMA).

In situ hybridization

In situ hybridization experiments were performed as described (Piotrowski and Nüsslein-Volhard, 2000). Probes used were for: *hand2* (Angelo et al., 2000), *edn1* (Miller et al., 2000), *myod* (Weinberg et al., 1996), *crestin* (Luo et al., 2001) and *fgf8* (Furthauer et al., 1997).

Confocal microangiography

Labeling of the blood vessels was performed essentially as described (Weinstein et al., 1995) with the following modifications: live, anesthetized 2.5 dpf larvae were mounted in 5% methylcellulose for fluorescent microsphere injections (Molecular Probes). The microspheres were injected into the yolk blood stream that flows into the heart. Images represent projections of *z*-series stacks that were taken within 15 minutes of the injection.

Transplantation experiments

Wild-type donor embryos were injected with 5% rhodamine-dextran and 3% lysine-fixable biotinylated-dextran (Molecular Probes) at the one- to two-cell stage (diluted in 0.2 mM KCl). Cells were transplanted into the animal pole of unlabeled embryos derived from heterozygous *vgo* parents at the late blastula stage. Larvae were scored for neural crest and ear clones on day 3 using a BioRad confocal microscope.

edn1 rescue experiments and cartilage rescue experiments

Donor embryos were injected with 2 pg activated Taram A/Alk4 (Tar*) at the one-cell stage to convert most of the donor cells to an endodermal fate (Peyrieras et al., 1998). As lineage tracers, we used 2.5% Alexa rhodamine-dextran and 2% biotinylated-dextran dissolved in 0.2 mM KCl. Donor cells were transplanted at the late blastula stage into the margin of unlabeled embryos derived from heterozygous *vgo/tbx1* parents. For transplantation, we used an air-filled standard 10 ml plastic syringe. At 24 hpf, the embryos were scored for endodermal clones under a fluorescent microscope. Embryos with endodermal clones were fixed with 4% paraformaldehyde overnight and processed for in situ hybridization with *edn1*. The transplanted cells were visualized using a avidin-biotinylated enzyme complex (ABC kit, Vector Laboratories) (Moens and Fritz, 1999). The embryos were mounted ventral side upwards under bridged cover slips after the yolk and the tail were removed. Subsequently the specimens were dehydrated in 100% methanol and cleared in a 1:2 solution of benzyl-benzoate: benzyl-alcohol. They were then photographed on a Zeiss Axiophot using a digital camera (Prog-Res/Kontron).

Results

Phenotype of *vgo* mutants

Zebrafish larvae homozygous for either of two existing *vgo* mutant alleles (*tm208* and *tu285*) die 6 to 7 days postfertilization (dpf) and appear to have the same phenotypic strength; the mutation is entirely recessive. At 4 dpf, *vgo* mutants lack segmentation of the posterior pharyngeal arches and have small otic vesicles (Piotrowski and Nüsslein-Volhard, 2000). Alcian Blue staining reveals that neural crest-derived cartilages are reduced (Fig. 1A-C) and often fused (Piotrowski and Nüsslein-Volhard, 2000). The severity of the phenotype depends on the genetic background. In the Tübingen background (in which *vgo* was first isolated), the first or mandibular arch is rarely affected, whereas in the AB* background it is always highly reduced (Fig. 1C). In the neurocranium surrounding the notochord (Fig. 1B, red elements), the parachordals (pc) are malformed and often not joined to the more anteriorly located neural crest-derived trabeculae, as in wild-type larvae (compare Fig. 1B,D). In addition, pharyngeal muscles associated with posterior arches are undetectable with molecular muscle markers such as *myod* (Piotrowski and Nüsslein-Volhard, 2000).

In this study, we investigated the aortic arch defects in *vgo*

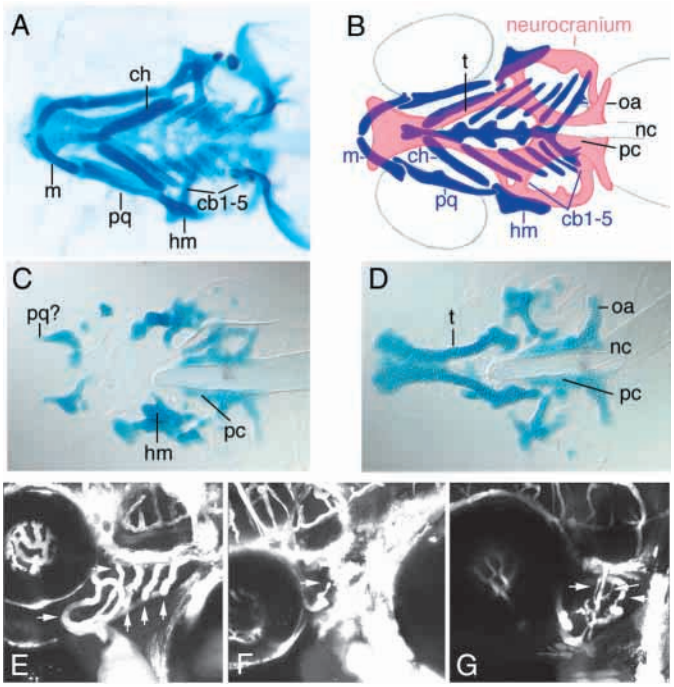

Fig. 1. Craniofacial and aortic arch phenotype in *vgo* (*tu285* allele, AB* background). (A) Alcian Blue cartilage preparation of a 5 dpf wild-type larva, ventral view. (B) Schematic drawing of the cartilages in A (blue, pharyngeal skeleton; red, neurocranium). (C) Dissected pharyngeal cartilages of a 5 dpf *vgo* larva. The cartilages in the mandibular (m, pq) and hyoid (ch, hm) arches are drastically reduced and the pharyngeal arches 3-7 (cb1-5) are completely absent. (D) Ventral view of the dissected neurocranium in a *vgo* larva. The mesodermally derived parachordalia (pc) are malformed and the anterior pole of the notochord (nc) extends almost to the point where the trabeculae (t) fuse. cb1-5, ceratobranchial cartilages 1-5; ch, ceratohyal cartilage; hm, hyomandibula; m, Meckel's cartilage of mandibular arch; nc, notochord; oa, occipital arch; pq, palatoquadrate; pc, parachordalia; t, trabeculae. (E-G) Aortic arches of 2.5 dpf larvae visualized with fluorescent microbeads. (E) Wild-type larva. At this stage, five aortic arches are visible (arrows). (F,G) *vgo* mutants showing variable reductions of the aortic arches. (F) Only one interrupted aortic arch is present (arrow). (G) Only three aortic arches formed but are much smaller in diameter than wild-type aortic arches (arrows).

in more detail by injecting fluorescent microspheres into the blood stream (Fig. 1E-G). Unlike mice or humans, in zebrafish the four posterior aortic arches of the gills persist into adulthood and only the two anterior ones become remodeled (Isogai et al., 2001) (http://eclipse.nichd.nih.gov/nichd/lmg/redirect.html). However, in 100% of *vgo* mutant larvae, the aortic arches are highly reduced and in most specimens only one or two aortic arches form and carry blood (Fig. 1F, arrows). Some mutant larvae have two or three aortic arches, frequently smaller in size (Fig. 1G, arrow). The morphologies of the most severely affected arches vary between individual larvae, making their identities difficult to determine. In several specimens, we also observed an ectopic connection or shunt between the oxygenated blood flowing through the aortic arches and oxygen-depleted venous blood flowing back to the heart (data not shown).

vgo represents a null allele of *tbx1*

Zebrafish *tbx1* cDNA encodes an open reading frame of 460 amino acids with extensive sequence similarity to mouse *Tbx1* (AF326960) (68.5% overall identity, 98.3% identity within the T-box; Fig. 2A). In addition, the exon-intron structure was identical to that of the mouse gene (data not shown).

Based on phenotypic similarities between *vgo* and *Tbx1* mutant mice, we tested *tbx1* as a candidate gene for *vgo*. Both *vgo*^{tm208} and *tbx1* mapped on linkage group 5 (LG5) in meiotic and radiation hybrid panels between markers z7351/fb38h03 and z10456 (Fig. 2B). Sequence analysis of *tbx1* in *vgo*^{tm208} revealed an A to T transition at nucleotide position 877 (arrow), which replaces an arginine (AGA) with a stop codon (TGA) near the end of the T-box, leading to the deletion of the entire C-terminus of the protein (Fig. 2C). In many T-box genes, such as *Brachyury/T* and *Tbx2* of the mouse, the effector domains are found in the C-terminal region of the protein (Carreira et al., 1998; He et al., 1999; Kispert et al., 1995), and thus *vgo*^{tm208} probably represents a null allele of *tbx1*. This mutation also leads to the loss of an *Alw*N1 restriction site, and this loss co-segregated with the *vgo* phenotype in 620 homozygous embryos. We also tested 100 recombinants for the flanking markers z7351 and z6371 that were among 1457 *vgo*^{tm208} embryos used in meiotic mapping and found that the loss of restriction site co-segregated with the mutation in all of these embryos as well. Based on these results, the calculated distance between this mutation and *vgo* is less than 0.03 cM, consistent with *vgo*^{tm208} being a mutation in *tbx1*. The *tbx1* sequence from the other allele (*vgo*^{tu285}) also harbors a mutation that introduces a premature stop codon. The mutation is a C to T transversion at the nucleotide position 364 (arrow), which deletes 98% of the T-box as well as the whole C terminus of the protein (Fig. 2C). Thus, both alleles of *vgo* appear to be null mutations in *tbx1*. However, the dose sensitivity of T-box genes (Hatcher and Basson, 2001; Nikaido et al., 2002) might explain our failure to convincingly rescue *vgo* by microinjection of *tbx1* cDNA or mRNA.

Zebrafish *tbx1* is expressed in the ear and in mesendodermal components of pharyngeal arches

Expression of zebrafish *tbx1* starts at the beginning of gastrulation (6 hpf) in the involuting cells within the hypoblast (Fig. 3A). These *tbx1*-expressing cells are likely to be the progenitors of the cranial paraxial mesendoderm. Between 6- and 10-somite stages, *tbx1* expression is found in parachordal mesendoderm as well as in a pair of bilateral stripes on either side of the neural tube that correspond to the cranial paraxial mesoderm, which extends from just posterior to the eyes (midbrain level) to approximately the level of rhombomere 6 (Fig. 3B,C). At the 20-somite stage, expression is detected in the primordia of the pharyngeal arches (Fig. 3D, p1-p7). By 27 hpf, expression is localized to the mesodermal core of the pharyngeal arches as well as to the arch epithelium, but not to neural crest cells lying in between (Fig. 3E). At 30 hpf, pharyngeal expression marks elongated cell clusters in each arch, which prefigure the forming arch muscles and possibly also mesenchyme cells surrounding the aortic arches (Fig. 3F). These patches are separated by the endodermal pouches that also express *tbx1*, which are more clearly observed in horizontal sections (Fig. 3G; 'e'). From 48 hpf onwards, *tbx1* expression is seen in individual arch muscles, which co-express

A

```
zebrafish tbx1  LWDEFNQLGTEMIVTKAGRRMFPTFQVKIFGMDPMADYMLLMDFLPVDDKRYRYAFHSSS
mouse Tbx1      LWDEFNQLGTEMIVTKAGRRMFPTFQVKLFGMDPMADYMLLMDFVPVDDKRYRYAFHSSS
chicken Tbx5    LWLKFHEVGTEMIITKAGRRMFPSYKVKVTGLNPKTKYILLMDIVPADD--HRYKFADNK
human TBX6      LWKEFSSVGTEMIITKAGRRMFPACRVSVTGLDPEARYLFLLDVIPVDG--ARYRWQGRR
Xenopus T       LWTRFKELTNEMIVTKNGRRMFPVLKVSMSGLDPNAMYTVLLDFVAADN--HRWKYVNGE

zebrafish tbx1  WLVAGKADPATPGRVHYHPDSPAKGAQWMKQIVSFDKLKLTNNLLDDNGHIILNSMHRYQ
mouse Tbx1      WLVAGKADPATPGRVHYHPDSPAKGAQWMKQIVSFDKLKLTNNLLDDNGHIILNSMHRYQ
chicken Tbx5    WSVTGKAEPAMPGRLYVHPDSPATGAHWMRQLVSFQKLKLTNNHLDPFGHIILNSMHKYQ
human TBX6      WEPSGKAEPRLPDRVYIHPDSPATGAHWMRQPVSFHRVKLTNSTLDPHGHLILHSMHKYQ
Xenopus T       WVPGGKPEPQAPSCVYIHPDSPNFGAHWMKDPVSFSKVKLTNKMNG-GGQIMLNSLHKYE

zebrafish tbx1  PRFHVVYVDPRKDSEKYAEEN--YKTFVFEETRFTAVTAYQNHRITQLKIASNPFAKGFR
mouse Tbx1      PRFHVVYVDPRKDSEKYAEEN--FKTFVFEETRFTAVTAYQNHRITQLKIASNPFAKGFR
chicken Tbx5    PRLHIVKAD---ENNGFGSKNTAFCTHVFPETAFIAVTSYQNHKITQLKIENNPFAKGFR
human TBX6      PRIHLVRAA-QLCSQHWGG----MASFRFPETTFISVTAYQNPQITQLKIAANPFAKGFR
Xenopus T       PRIHIVRVG---GTQRMIT------SHSFPETQFIAVTAYQNEEITALKIKHNPFAKAFL
```

B

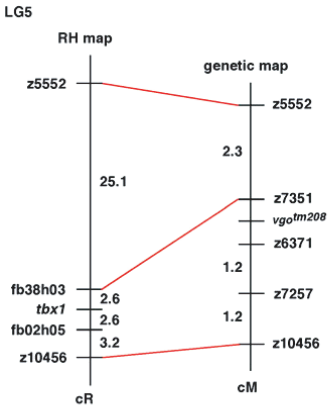

C

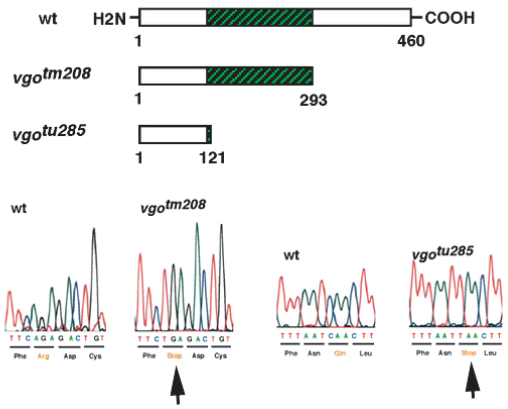

Fig. 2. Linkage between *tbx1* and *vgo*^{tm208}. (A) Amino acid sequence alignment of zebrafish *tbx1* and other T-box genes. Residues identical to zebrafish *tbx1* are in gray. Only T-domain sequences are shown. (B) Physical and genetic maps of linkage group 5 (LG5) showing map positions of *tbx1* and *vgo*^{tm208}. (C) Sequence analysis of *tbx1* in wild-type (wt), *vgo*^{tm208} and *vgo*^{tu285} mutants. Box diagrams represent conceptual products of translation of *tbx1* cDNAs from wild type, *vgo*^{tm208} and *vgo*^{tu285}. T-box region is shown by hatched boxes. Note that the A to T transition in *vgo*^{tm208} eliminates the *Alw*NI recognition sequence (CAGNNNCTG).

myod at this stage (Fig. 3H,I; arrows) and in endodermal pouches separating individual arches.

tbx1 is also strongly expressed throughout the morphogenesis of the zebrafish ear, correlating with the ear defects observed in *vgo* mutants. Expression in the otic vesicles begins at approximately the eight-somite stage and persists in 72 hpf larvae (Fig. 3C,D,J-L). *tbx1* is initially expressed throughout the ear epithelium (Fig. 3J) as well as in the apical poles of the cells within the sensory patches (christae, Fig. 3K,L; asterisks) and semicircular canals (Fig. 3K,L; arrows). Expression is absent in the anteroventral pole of the otocyst (Fig. 3J, arrow), which may correspond to the primordium of the anterior macula, the only sensory patch that forms in the *vgo* mutant.

vgo/tbx1 is required non-cell autonomously in neural crest cells and cell autonomously in the ear

As *vgo/tbx1* mutants exhibit defects in the neural crest-derived head skeleton where *tbx1* is not expressed, we tested whether *vgo/tbx1* is required within the surrounding mesendoderm. We attempted to rescue *vgo/tbx1* mutant cartilages (AB* background) by placing wild-type cells into the pharyngeal mesendoderm. Transplantation of unmanipulated wild-type cells usually results in small mesendodermal clones. To achieve larger clone sizes in the pharynx, we injected the wild-type donors prior to transplantation with Tar*, an activated version of the type 1 TGFβ-related receptor Taram-A (Tar) (David and Rosa, 2001; David et al., 2002; Peyrieras et al., 1998). Tar is normally expressed in endodermal precursor cells and injection of its activated form converts blastomeres to an endodermal fate. Tar*-injected cells behave like endogenous endodermal cells in transplantation experiments (David and Rosa, 2001; Peyrieras et al., 1998; Renucci et al., 1996). Relevant to our experiments is the fact that transplanted cells do not induce ectopic expression of downstream nodal targets (David and Rosa, 2001). As expected, donor cells in the mosaic host embryos contribute largely to the pharynx, endodermal pouches of the pharyngeal arches and the digestive tract. In 12 out of 43 *vgo* larvae (28%) in which transplanted wild-type cells contributed to the mesendoderm of the pharyngeal arches, we observed partial rescue of the neural crest-derived pharyngeal cartilages (Fig. 4A,B). Rescue was generally unilateral, corresponding to the side to which most transplanted cells contributed, and in separate cases included restoration of cartilages in the mandibular (Fig. 4B, n=5), hyoid (Fig. 4A,B; n=3) and branchial arches (Fig. 4A; n=4). These results suggest that cartilage defects in *vgo/tbx1* result from defective signaling from the endoderm.

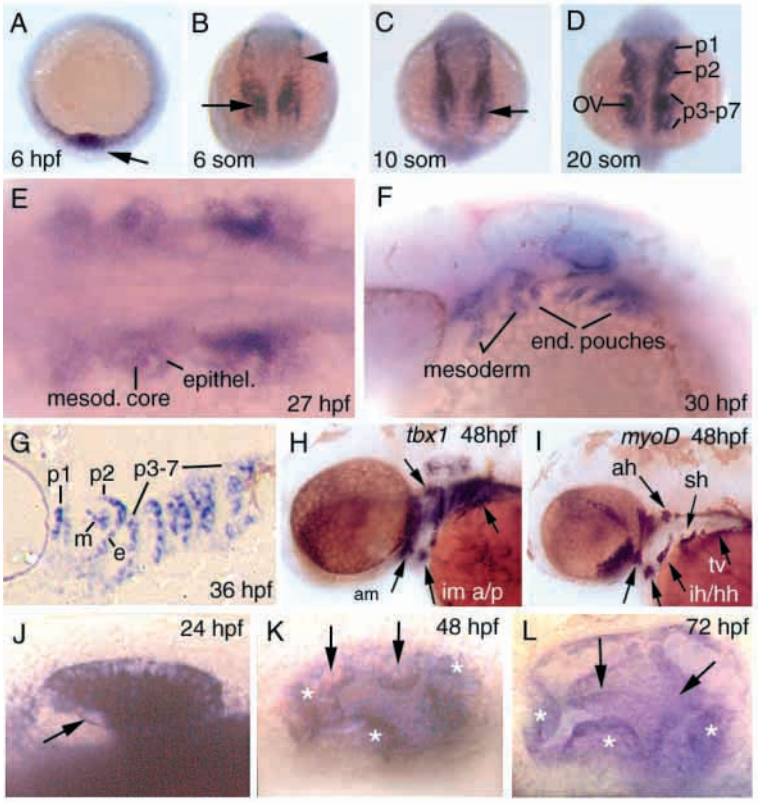

Fig. 3. Expression of *vgo/tbx1* during zebrafish embryogenesis. (A) Animal pole view. (B-E,G) Dorsal views and (F,H-L) lateral views. (A) In a shield stage embryo (6 hpf), expression is confined to the hypoblast cells of the shield (arrow) and flanking region. (B) Six-somite stage (12 hpf). Expressing cells are now organized into the cranial paraxial mesoderm (thin lateral stripe, marked by an arrowhead) and a more medial group of mesenchyme cells consisting of prospective pharyngeal endodermal cells and cells of parachordal mesoderm (arrow). (C) Ten-somite stage (14 hpf). New expression commences within the otic placode (arrow). (D) Twenty-somite stage (19 hpf). *vgo/tbx1*-expressing cells are now organized into the primordia of the pharyngeal arches (p1-p7). OV, otic vesicle. (E) 27 hpf. *vgo/tbx1* expression within the mesodermal core and endodermal epithelia of individual arches. Anterior towards the left. (F) Lateral view of *vgo/tbx1* expression in a 30 hpf embryo. In the anterior arches, the mesodermal core is in focus. In the posterior arches, the endodermal pouches are visible. (G) Horizontal section through the pharyngeal region of a 36 hpf embryo. The endodermal pouches (e) and mesodermal cores (m) of the arches are clearly *vgo/tbx1* positive. (H,I) *tbx1* is expressed in pharyngeal arch muscles. (H) At 48 hpf, *vgo/tbx1* is expressed in most of the pharyngeal arch muscles that also express *myod* (I). (J-L) High magnification views of *vgo/tbx1* expression within the otic vesicle. (J) 24 hpf. (K) 48 hpf. (L) 72 hpf. Expression is initially found throughout the otic vesicle except for the anteroventral corner (arrow in J). Strong expression is maintained in the developing cristae (asterisks in K,L) and semicircular canals (arrows in K,L). ah, adductor hyoideus; am, adductor mandibulae; ih, interhyoideus; hh, hyohyoideus; ima, intermandibularis anterior; imp, intermandibularis posterior; sh, sternohyoideus; tv, transversus ventralis.

In another set of experiments we observed that non-Tar*-injected transplanted wild-type cells occasionally contributed to the semicircular canals of just one ear of the mutant embryo (Fig. 4C), leading to an increase in ear size at 5dpf (Fig. 4E; 7/21=30%). The semicircular canals on the contralateral side that did not receive wild-type cells remained small (Fig. 4D). This indicates that in contrast to neural crest cells, cells in the semicircular canals require *vgo/tbx1* cell-autonomously to develop properly.

Regulatory interactions between *vgo/tbx1*, *edn1* and *hand2*

Edn1 and *Hand2* (previously known as *dHand*) are expressed in the pharyngeal arches and cause phenotypes similar to DGS if knocked-out in mice (Kurihara et al., 1995; Kurihara et al., 1994; Srivastava et al., 1997; Thomas et al., 1998) or mutated in zebrafish (Miller et al., 2000). *Edn1* is a small signaling peptide which regulates *Hand2* (called *hand2* in zebrafish), a bHLH transcription factor expressed in the neural crest cells surrounding the mesodermal core of the arches (Charite et al., 2001; Miller et al., 2000). In both mouse and zebrafish, *edn1* is expressed in a similar pattern to *tbx1*, in pharyngeal arch epithelia (both surface ectoderm and pharyngeal endoderm) and in the mesodermal core (Fig. 3E, Fig. 5A). This prompted us to test whether *vgo/tbx1*, *edn1* and *hand2* interact in a regulatory pathway. The existence of zebrafish mutants with mutations in all three genes (*vgo/tbx1*, *suc/edn1*, and *han/hand2*) facilitates the study of their epistatic relationships.

In situ hybridization experiments revealed that *edn1* expression is strongly reduced in *vgo/tbx1* mutants, particularly in the posterior arches (Fig. 5A,B). This lack of expression is not due to the lack of cells that normally express *edn1*, as mesenchymal cells and the ectodermal lining of the pharyngeal arches, where *edn1* is normally expressed, are present in the posterior arches of *vgo* mutant embryos (Piotrowski and Nüsslein-Volhard, 2000). In addition, *edn1* and *tbx1* are co-expressed in the pharyngeal arches (Fig. 3E, Fig. 5A,C,E). Even though disorganized, *tbx1* mRNA persists in cells of the pharyngeal arches of *vgo* mutant embryos up to ~28 hpf (Fig. 5C,D), whereas *edn1* expression in *vgo* mutants is reduced or absent in these cells (Fig. 5E,F). This demonstrates that many cells that normally express *edn1* are still present in *vgo*, yet fail to express *edn1* when *tbx1* is mutated.

In *vgo/tbx1* mutants, the expression of *hand2* in neural crest cells is reduced in the two anterior pharyngeal arches and absent in the posterior arches (Fig. 5G,H). However, expression in the cardiac mesoderm and fin buds is unaffected, supporting studies showing that *Hand2* expression is controlled by different enhancers in these two regions (Charite et al., 2001; Thomas et al., 1998). Defects in *hand2* expression in *vgo/tbx1* mutants again are not simply due to the absence of neural crest cells, as in situ hybridization experiments with *crestin*, a pan-neural crest marker (Luo et al., 2001; Rubinstein et al., 2000) shows the presence of neural crest cells even posterior to the otic vesicle of mutant embryos (Fig. 5I,J, arrows).

Therefore, reductions in *edn1* and *hand2* expression in *vgo/tbx1* mutants are probably due to gene regulation defects. A simple regulatory cascade in which *vgo/tbx1* is upstream of *edn1* and *hand2* predicts that *vgo/tbx1* expression is unaffected in *edn1/suc* and *hand2*/*han* mutant embryos, which is indeed

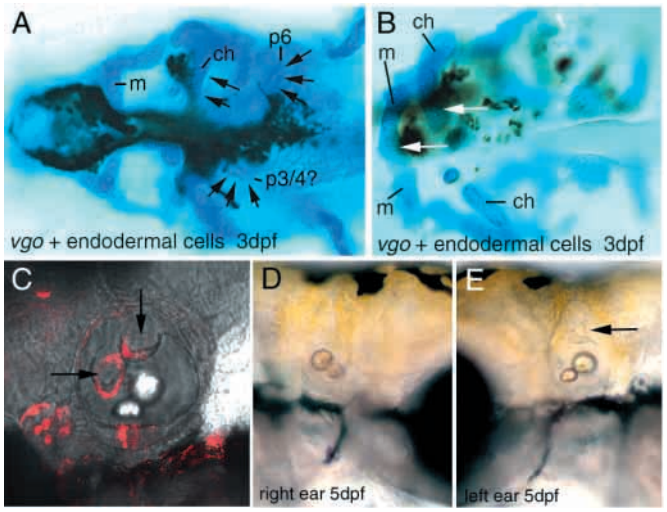

Fig. 4. Cell transplantation experiments between wild-type and *vgo/tbx1* larvae (*tm208* allele). (A,B) Ventral views of 3 dpf *vgo/tbx1* larvae stained with Alcian Blue, showing the rescue of cartilages (arrows) in the vicinity of transplanted *Tar**-expressing wild-type cells (black staining). (A) p6 is rescued only on the left side of the embryo and is absent on the contralateral side. (B) m and ch cartilages are rescued on the left side, judged by their shape and cell number compared with the contralateral side. (C) Lateral view of left ear of a 3 dpf *vgo/tbx1* larva. Transplanted wild-type cells (in red fluorescence) contributed to the developing semicircular canals (arrows). (D,E) The same larva as in C at 5 dpf. Wild-type cells were able to partially restore ear size and the presence of semicircular canals (arrow) in the left ear (E), whereas the right ear, which did not receive any wild-type cells, remained small (D) and without semicircular canals. cb1-5, ceratobranchial cartilages 1-5; ch, ceratohyal cartilage; hm, hyomandibula; m, Meckel's cartilage of mandibular arch; nc, notochord; oa, occipital arch; pq, palatoquadrate; pc, parachordalia; t, trabeculae.

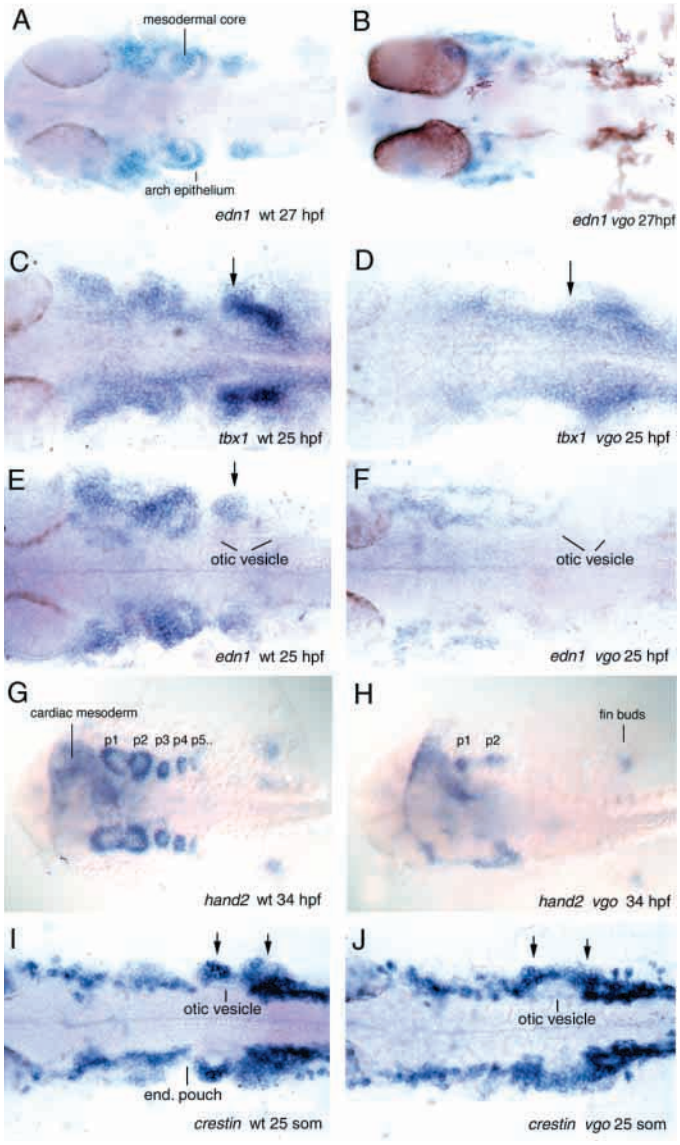

Fig. 5. Expression of *vgo/tbx1* pathway genes in mutants. Ventral views with anterior towards the left in all panels. (A,B) Expression of *edn1* in wild-type (A) and *vgo/tbx1* (B) 27 hpf embryos. (C,D) Expression of *tbx1* in 25 hpf wild-type (C) and *vgo/tbx1* (D) embryos. In *vgo/tbx1* embryos, *tbx1* mRNA is still present in cells ventral to the otic vesicle (Fig. 5D, arrows). At this stage, the otic vesicle in *vgo* embryos no longer express *tbx1*. (E,F) *edn1* expression in 25 hpf wild-type (E) and *vgo/tbx1* (F) embryos. In *vgo/tbx1* embryos, *edn1* expression is very much reduced in cells immediately anterior to the otic vesicle. The downregulation of *edn1* in the arches is not due to the absence of cells, as *tbx1*-expressing cells are present (D). (G,H) Expression of *hand2* in 34 hpf wild-type (G) and *vgo/tbx1* (H) embryos. (I,J) Expression of *crestin* in 20-somite wild-type (I) and *vgo/tbx1* (J) embryos. Absence of *hand2* expression in the posterior arches of *vgo/tbx1* embryos is not caused by the absence of neural crest cells, as revealed by the pan-neural crest marker *crestin* in *vgo/tbx1* embryos (J). Arrows indicate neural crest cells ventral and posterior to the otic vesicle.

the case (Fig. 6A,B). In addition, *hand2* is downregulated in *edn1/suc* mutants (Miller et al., 2000), whereas in *hand2/han* mutants, *edn1* expression is normal (Fig. 6C). The results of these in situ hybridization experiments suggest that *vgo/tbx1* acts upstream of *edn1* and *hand2*.

A conditional knockout of *Fgf8* in mouse has demonstrated that in the mandibular arch *Edn1* is regulated by *Fgf8* (Trumpp et al., 1999; Tucker et al., 1999). In zebrafish, we did not detect a regulation of *edn1* by *fgf8*, as *edn1* expression is normal in *fgf8* mutant *acerebellar* embryos *(ace*) (Reifers et al., 1998) (data not shown). In mice, it has also been shown that *Fgf8* acts downstream of *Tbx1* (Vitelli et al., 2002). We analyzed *fgf8* expression in *vgo/tbx1* mutants (*vgo*^{tm208} and *vgo*^{tu285}, AB* background). However, in zebrafish, no alterations of *fgf8* expression were detected (Fig. 6D) suggesting that *fgf8* is not downstream of *vgo/tbx1*. We also tested whether *fgf8* might be upstream of *vgo/tbx1*. However, *tbx1* expression is normal in *ace/fgf8* mutants, suggesting that *fgf8* is not upstream of *vgo/tbx1* (Fig. 6E,F). Thus, it is likely that in zebrafish other Fgf genes are functionally redundant with *fgf8* in pharyngeal arch development.

Endodermal *vgo/tbx1*-expressing cells induce *edn1*

To confirm the result from the in situ hybridization experiments, we tested if *vgo/tbx1* regulates *edn1* by transplanting wild-type endodermal cells at the blastula stage into *vgo/tbx1* mutants. In three out of 20 *vgo/tbx1* mutants that had transplanted cells in the pharynx, we observed

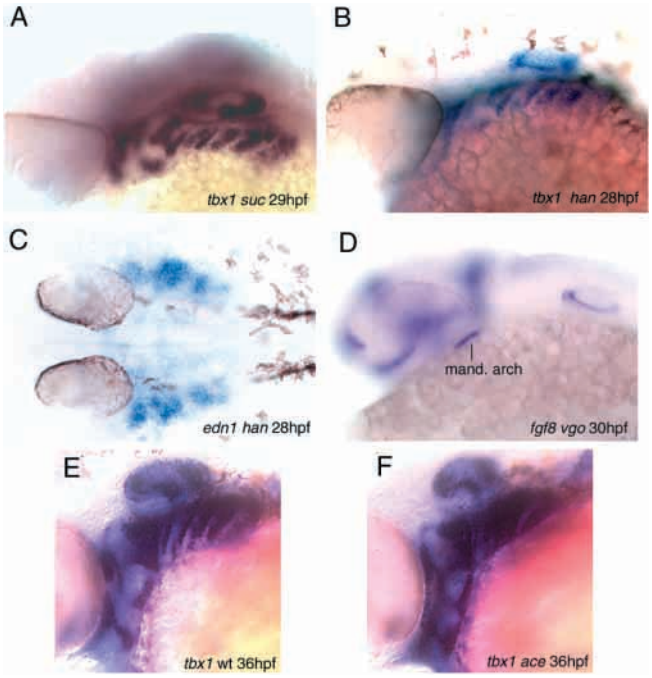

Fig. 6. Expression analysis of *tbx1*, *edn1* and *fgf8* in mutants. (A,B) Expression of *vgo/tbx1* in 29 hpf *suc* (A) and 28 hpf *han* (B) embryos. (C) Expression of *edn1* in *han* embryos. (D) *fgf8* expression in the mandibular arch of *vgo/tbx1* (30 hpf). (E,F) *vgo/tbx1* expression in 36 hpf wild-type (E) and *ace* (F) embryos.

upregulation of *edn1* (Fig. 7B). However, transplantation of cells at this early stage leads to small mesendodermal clones, because many cells also contribute to the ectoderm. The small number of transplanted endodermal cells in *vgo/tbx1* mutants might explain why we only observed rescue of *edn1* expression in a relatively low number of mutant embryos. Therefore, we also transplanted Tar*-injected wild-type cells into *vgo* mutants to ensure that the transplanted cells contributed to the endoderm. In this experiment, 119 embryos received transplanted cells in the pharyngeal region. Among these were 34 *vgo/tbx1* mutants, out of which 32 showed an increase in the expression level of *edn1* close to the transplanted cells (94.7%, Fig. 7C, arrows indicate transplanted cells). In many embryos, *edn1* expression was not only detected in the transplanted cells themselves but also in several tiers of cells adjacent to the transplanted cells. As *vgo/tbx1* is a transcription factor, an intermediate gene product must exist that transduces the signal over several cell diameters. Consequently, our data suggests that *vgo/tbx1* is regulating *edn1* indirectly, although we cannot rule out that *vgo/tbx1* also is regulating *edn1* directly in a subset of cells.

Discussion

vgo encodes *tbx1*

In this report, we show that the *vgo* mutation affects the zebrafish *tbx1* gene. In *vgo* mutant embryos, pharyngeal pouches 2-6 do not develop, the pharyngeal cartilages of the different pharyngeal arches fuse with each other, thymus development is impaired and the ear remains very small. With the exception of the ear defect, all other defects can be attributed to abnormal development of the pharyngeal endoderm, specifically to defective endodermal pouch development (Piotrowski and Nüsslein-Volhard, 2000). In agreement with the mutant phenotype, *tbx1* is expressed in cranial paraxial mesoderm, pharyngeal endoderm, the mesenchyme surrounding the aortic arches and in the otic vesicle, all of which are disrupted in *vgo* mutants. The homozygous phenotype of zebrafish *vgo* mutants closely resembles the phenotypes of individuals with DiGeorge Syndrome (DGS), including craniofacial, thymic, aortic arch and ear defects (Ryan et al., 1997). Even though a deletion that includes *Tbx1* accounts for most malformations in the DGS, not all patients carry a mutation in that gene (Lindsay, 2001), and mutations in several other genes cause phenotypes associated with DGS. Nevertheless, recent studies in mice have shown that *Tbx1* is one of the main candidates for causing the aortic arch phenotype in DGS (Jerome and Papaioannou, 2001; Lindsay et al., 2001; Merscher et al., 2001). An important difference between the different species is that DGS is caused by heterozygous deletions in humans, and in mice homozygous null mutations in *Tbx1* lead to an almost complete set of DGS-like phenotypes whereas only the aortic arch phenotype is observed in heterozygotes. By contrast, *vgo* is a recessive gene in zebrafish and no phenotype is observed in the heterozygous embryos. T-box genes have been shown to be dose sensitive (Hatcher and Basson, 2001) and different sensitivities to *Tbx1*

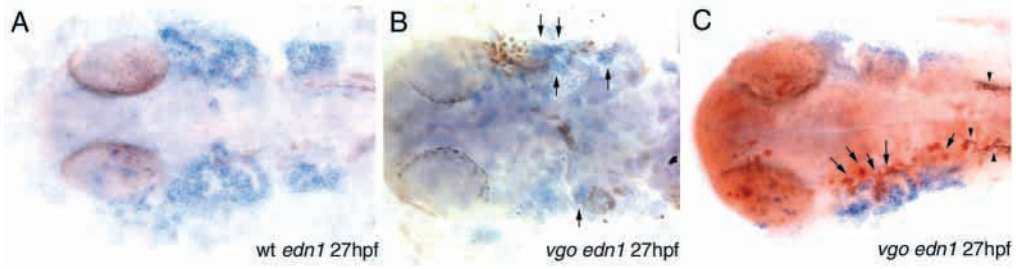

Fig. 7. Rescue of *edn1* expression by transplanted endodermal cells in *vgo/tbx1* embryos. Transplanted cells in brown (labeled with biotin) and *edn1* expression in blue. (A) Expression of *edn1* in a 27 hpf wild-type control embryo. (B) *vgo/tbx1* host embryo in which transplanted wild-type cells induced upregulation of *edn1* (arrows). (C) *vgo/tbx1* host embryo, in which Tar*-injected endodermal cells contributed to the pharynx on only one side. On the control side, *edn1* expression is weak and disorganized. The side that received endodermal cells (brown cells, arrows) shows much stronger expression of *edn1*, which includes cells located several cell diameters away from the transplanted cells (arrowheads point at pigment cells). Flat mounts in dorsal views with anterior towards the left in all panels.

dose may account for these differences. Nevertheless, given the similarity of the observed defects, both the mouse and the zebrafish models present valuable opportunities for the study of DGS.

vgo/tbx1 function in the endoderm is required for normal development of neural crest-derived pharyngeal structures

In our description of the *vgo* mutant phenotype, we hypothesized that the neural crest defects are secondary to defects in the pharyngeal endoderm (Piotrowski and Nüsslein-Volhard, 2000). This suggestion is supported by the expression pattern of *tbx1*, which is not expressed in neural crest cells. Furthermore, we showed that transplantation of wild-type endodermal cells can rescue cartilage formation in *vgo/tbx1* mutants. The fact that neural crest induction and migration appear normal in *vgo* (Piotrowski and Nüsslein-Volhard, 2000) also supports this conclusion. These three results suggest that the mesendoderm is the source of a secreted signal required for the proper differentiation of neural crest cells in the pharyngeal arches.

DGS often has been described as being caused by autonomous defects in the development of neural crest cells, an explanation supported by the fact that neural crest ablation in chicks results in very similar phenotypes, as have been reported for DGS. By contrast, similar to our findings in *vgo/tbx1* mutant fish, a study in *Tbx1*$^{-/-}$ mice suggests that neural crest defects are indirect (Kochilas et al., 2002). However, as *TBX1* is not the only gene responsible for causing DGS, downstream targets of *TBX1* that are expressed in neural crest cells may also represent candidate genes for causing DGS. In contrast to what we found for neural crest cells, we have demonstrated that *vgo/tbx1* is required cell autonomously in the outgrowing semicircular canals of the ear. Therefore, *TBX1* may not only be responsible for the pharyngeal arch defects characteristic of DGS but also for the ear defects found in these individuals (Reyes et al., 1999; Funke et al., 2001).

Genetic components of the *tbx1* pathway in the pharyngeal arches

A large number of genes are expressed in the pharyngeal arches, underscoring the genetic complexity of their development (Garg et al., 2001). *vgo/tbx1* appears to be one of the earliest genes involved in this process as disruption of its function affects the segmentation of the endodermal pouches (Piotrowski and Nüsslein-Volhard, 2000), which is one of the earliest events in arch morphogenesis. In mice and chickens, *Shh* (Garg et al., 2001; Yamagishi et al., 2003), *Fgf8* (Frank et al., 2002; Vitelli et al., 2002) and *Vegf* (Stalmans et al., 2003) have been suggested to be part of the *Tbx1* pathway.

Among genes implicated in DGS and in pharyngeal development, zebrafish mutations have been isolated in *fgf8*, *tbx1*, *edn1* and *hand2*, and therefore we focused our study on these loci. Our experiments suggest regulatory interactions between the *tbx1* and the *edn1* pathways. In mice, such a relationship might not exist, as *Edn1* expression has been reported to be normal in the aortic arch endothelial cells of *Tbx1*$^{-/-}$ animals (Kochilas et al., 2002). However, expression of *Edn1* in the pharyngeal arches of *Tbx1*$^{-/-}$ mice has not been directly tested. In zebrafish, transplantation of wild-type cells into *vgo/tbx1* mutant embryos showed a clear increase in *edn1* expression in the pharynx in cells close to the transplanted cells (Fig. 7B,C). The fact that *edn1* expression was also induced in cells up to several cell diameters away from the transplanted cells implies that *tbx1* regulates one or several intermediate factors that in turn regulate *edn1*, possibly in addition to direct regulation in certain cell types.

We found that gene regulation within the anterior and posterior arches differs slightly (Fig. 8C). This result is not surprising, given that most jaw mutants mainly affect either the anterior or the posterior arches (Piotrowski et al., 1996; Schilling et al., 1996). A model for genetic interactions between *vgo/tbx1*, *edn1* and *hand2* in the pharyngeal arches and a summary of expression data are presented in Fig. 8. Within the first arch of the mouse, *Edn1* has been shown to be regulated by *Fgf8* (Trumpp et al., 1999; Tucker et al., 1999), and *Tbx1* and *Fgf8* have been shown to interact genetically (Funke et al., 2001; Vitelli et al., 2002). In

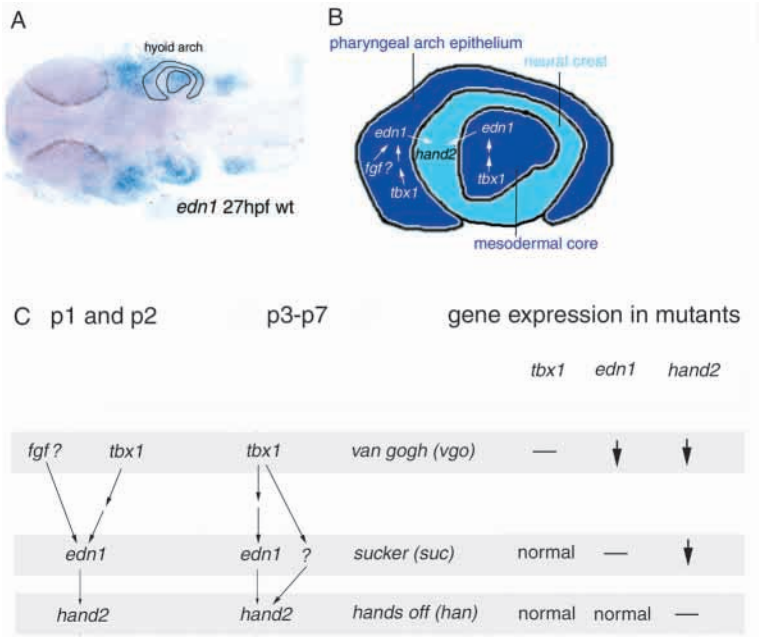

Fig. 8. Model of the genetic pathway regulating development of the anterior and posterior pharyngeal arches in zebrafish. (A) *edn1* expression in 27 hpf wild-type embryo and (B) schematic drawing of the *tbx1* pathway in an arch primordium (dark blue, pharyngeal arch epithelium and mesodermal core; light blue, neural crest cells). Outlined in black is the hyoid arch, exemplifying the distribution of *edn1*- and *tbx1*-positive cells within a developing arch. (C) Genetic pathway regulating development of the anterior and posterior arches and zebrafish mutants analyzed in this study with the expression of *tbx1*, *edn1* and *hand2* in these mutants. Dash indicates 'no data'. Mandibular (p1) and hyoid (p2) arches: *tbx1* regulates *edn1* within the arch epithelium and the mesodermal core. Within these arches, *edn1* is also possibly regulated independently by another gene, probably an Fgf. *edn1* in turn regulates the expression of *hand2* in the neural crest-derived cells surrounding the mesodermal core of the arch. In posterior arches (p3-7), *tbx1* is likely to be the major regulator of *edn1*. Downstream of *edn1*, *hand2* expression is likely to be controlled by *edn1*, as well as by *tbx1* via an as yet unknown signaling molecule ('?').

zebrafish, *fgf8* does not appear to regulate *edn1*, as *fgf8/ace* mutants (Reifers et al., 1998) do not show defects in *edn1* gene expression (data not shown). Likewise, *vgo/tbx1* does not appear to be upstream of *fgf8*, as *fgf8* expression is normal in *vgo/tbx1* mutants (Fig. 6F). Owing to gene duplication events, the zebrafish genome contains more redundant genes than mice, and it is possible that other Fgfs play a role in zebrafish pharyngeal arch development. This is likely because, in contrast to mice and chicks, in which *fgf8* is expressed in all endodermal pouches, *fgf8* is only expressed in the mandibular arch in zebrafish. Regulation of *edn1* by another member of the Fgf family may be responsible for the remaining, although reduced, *edn1* and *hand2* expression still present in the first arch of *vgo/tbx1* (Fig. 5B,H; see Fig. 8C).

Within the posterior arches, *vgo/tbx1* might play the dominant role in regulating *edn1*, as *edn1* expression is strongly reduced in the posterior arches of *vgo* mutant fish (Fig. 5B). We further suggest that in the posterior arches *hand2* is not only regulated by *edn1* but also by other genes, because in *suc/edn1* mutants, *hand2* expression is still detectable in this region (Miller et al., 2000). We hypothesize that *hand2* might also be regulated by *tbx1* independently of *edn1* via an unknown intermediate gene ('?' in Fig. 8C). This hypothesis is supported by the finding that in *vgo/tbx1* mutants, *hand2* expression is strongly reduced in the posterior arches (Fig. 5H), whereas *suc/edn1* embryos still show expression (Miller et al., 2000).

In summary, the identification of *tbx1* as the gene responsible for the *vgo* mutation allows for mechanistic studies of pharyngeal development in zebrafish and adds a potentially useful model system to the available tools for understanding the etiology of DGS.

We thank F. Rosa, C. Miller and D. Yelon for kindly providing the Tar*, *edn1* and *hand2* constructs, respectively; B. Roman for teaching us how to perform microangiographies; members of the Dawid and Ho laboratories for helpful discussions; D. Grunwald for his support; and E. Laver and H. Dow for help with fish husbandry. We also thank A. Baldini for sharing data prior to publication and A. Sanchez Alvarado for critically reading the manuscript. This study was supported by a HFSP Long Term- and NIH visiting fellow fellowship to T.P.; a postdoctoral fellowship from the American Heart Association, Heritage Affiliate to D.A.; grants from the German Human Genome Project (DHGP Grant 01 KW 9919 and KW 9627/1) to R.G. and P.H.; and grants from the NIH and NSF to R.K.H.

References

Angelo, S., Lohr, J., Lee, K. H., Ticho, B. S., Breitbart, R. E., Hill, S., Yost, H. J. and Srivastava, D. (2000). Conservation of sequence and expression of Xenopus and zebrafish dHAND during cardiac, branchial arch and lateral mesoderm development. *Mech. Dev.* **95**, 231-237.

Bamshad, M., Lin, R. C., Law, D. J., Watkins, W. C., Krakowiak, P. A., Moore, M. E., Franceschini, P., Lala, R., Holmes, L. B., Gebuhr, T. C. et al. (1997). Mutations in human TBX3 alter limb, apocrine and genital development in ulnar-mammary syndrome. *Nat. Genet.* **16**, 311-315.

Basson, C. T., Bachinsky, D. R., Lin, R. C., Levi, T., Elkins, J. A., Soults, J., Grayzel, D., Kroumpouzou, E., Traill, T. A., Leblanc-Straceski, J. et al. (1997). Mutations in human TBX5 cause limb and cardiac malformation in Holt-Oram syndrome. *Nat. Genet.* **15**, 30-35.

Carreira, S., Dexter, T. J., Yavuzer, U., Easty, D. J. and Goding, C. R. (1998). Brachyury-related transcription factor Tbx2 and repression of the melanocyte-specific TRP-1 promoter. *Mol. Cell Biol.* **18**, 5099-5108.

Charite, J., McFadden, D. G., Merlo, G., Levi, G., Clouthier, D. E., Yanagisawa, M., Richardson, J. A. and Olson, E. N. (2001). Role of Dlx6 in regulation of an endothelin-1-dependent, dHAND branchial arch enhancer. *Genes Dev.* **15**, 3039-3049.

David, N. B. and Rosa, F. M. (2001). Cell autonomous commitment to an endodermal fate and behaviour by activation of Nodal signalling. *Development* **128**, 3937-3947.

David, N. B., Saint-Etienne, L., Tsang, M., Schilling, T. F. and Rosa, F. M. (2002). Requirement for endoderm and FGF3 in ventral head skeleton formation. *Development* **129**, 4457-4468.

Frank, D. U., Fotheringham, L. K., Brewer, J. A., Muglia, L. J., Tristani-Firouzi, M., Capecchi, M. R. and Moon, A. M. (2002). An Fgf8 mouse mutant phenocopies human 22q11 deletion syndrome. *Development* **129**, 4591-4603.

Funke, B., Epstein, J. A., Kochilas, L. K., Lu, M. M., Pandita, R. K., Liao, J., Bauerndistel, R., Schuler, T., Schorle, H., Brown, M. C. et al. (2001). Mice overexpressing genes from the 22q11 region deleted in velo-cardio-facial syndrome/DiGeorge syndrome have middle and inner ear defects. *Hum. Mol. Genet.* **10**, 2549-2556.

Furthauer, M., Thisse, C. and Thisse, B. (1997). A role for FGF-8 in the dorsoventral patterning of the zebrafish gastrula. *Development* **124**, 4253-4264.

Garg, V., Yamagishi, C., Hu, T., Kathiriya, I. S., Yamagishi, H. and Srivastava, D. (2001). Tbx1, a DiGeorge syndrome candidate gene, is regulated by sonic hedgehog during pharyngeal arch development. *Dev. Biol.* **235**, 62-73.

Griffin, K. J., Amacher, S. L., Kimmel, C. B. and Kimelman, D. (1998). Molecular identification of spadetail: regulation of zebrafish trunk and tail mesoderm formation by T-box genes. *Development* **125**, 3379-3388.

Haffter, P., Granato, M., Brand, M., Mullins, M. C., Hammerschmidt, M., Kane, D. A., Odenthal, J., van Eeden, F. J., Jiang, Y. J., Heisenberg, C. P. et al. (1996). The identification of genes with unique and essential functions in the development of the zebrafish, Danio rerio. *Development* **123**, 1-36.

Hatcher, C. J. and Basson, C. T. (2001). Getting the T-box dose right. *Nat. Med.* **7**, 1185-1186.

He, M., Wen, L., Campbell, C. E., Wu, J. Y. and Rao, Y. (1999). Transcription repression by Xenopus ET and its human ortholog TBX3, a gene involved in ulnar-mammary syndrome. *Proc. Natl. Acad. Sci. USA* **96**, 10212-10217.

Hukriede, N. A., Joly, L., Tsang, M., Miles, J., Tellis, P., Epstein, J. A., Barbazuk, W. B., Li, F. N., Paw, B., Postlethwait, J. H. et al. (1999). Radiation hybrid mapping of the zebrafish genome. *Proc. Natl. Acad. Sci. USA* **96**, 9745-9750.

Isogai, S., Horiguchi, M. and Weinstein, B. M. (2001). The vascular anatomy of the developing zebrafish: an atlas of embryonic and early larval development. *Dev. Biol.* **230**, 278-301.

Jerome, L. A. and Papaioannou, V. E. (2001). DiGeorge syndrome phenotype in mice mutant for the T-box gene, Tbx1. *Nat. Genet.* **27**, 286-291.

Kispert, A., Koschorz, B. and Herrmann, B. G. (1995). The T protein encoded by Brachyury is a tissue-specific transcription factor. *EMBO J.* **14**, 4763-4772.

Knapik, E. W., Goodman, A., Atkinson, O. S., Roberts, C. T., Shiozawa, M., Sim, C. U., Weksler-Zangen, S., Trolliet, M. R., Futrell, C., Innes, B. A. et al. (1996). A reference cross DNA panel for zebrafish (Danio rerio) anchored with simple sequence length polymorphisms. *Development* **123**, 451-460.

Kochilas, L., Merscher-Gomez, S., Lu, M. M., Potluri, V., Liao, J., Kucherlapati, R., Morrow, B. and Epstein, J. A. (2002). The role of neural crest during cardiac development in a mouse model of DiGeorge syndrome. *Dev. Biol.* **251**, 157-166.

Kurihara, Y., Kurihara, H., Oda, H., Maemura, K., Nagai, R., Ishikawa, T. and Yazaki, Y. (1995). Aortic arch malformations and ventricular septal defect in mice deficient in endothelin-1. *J. Clin. Invest.* **96**, 293-300.

Kurihara, Y., Kurihara, H., Suzuki, H., Kodama, T., Maemura, K., Nagai, R., Oda, H., Kuwaki, T., Cao, W. H., Kamada, N. et al. (1994). Elevated blood pressure and craniofacial abnormalities in mice deficient in endothelin-1. *Nature* **368**, 703-710.

Lindsay, E. A. (2001). Chromosomal microdeletions: dissecting del22q11 syndrome. *Nat. Rev. Genet.* **2**, 858-868.

Lindsay, E. A., Vitelli, F., Su, H., Morishima, M., Huynh, T., Pramparo, T., Jurecic, V., Ogunrinu, G., Sutherland, H. F., Scambler, P. J. et al. (2001). Tbx1 haploinsufficieny in the DiGeorge syndrome region causes aortic arch defects in mice. *Nature* **410**, 97-101.

Luo, R., An, M., Arduini, B. L. and Henion, P. D. (2001). Specific pan-

neural crest expression of zebrafish Crestin throughout embryonic development. *Dev. Dyn.* **220**, 169-174.

Merscher, S., Funke, B., Epstein, J. A., Heyer, J., Puech, A., Lu, M. M., Xavier, R. J., Demay, M. B., Russell, R. G., Factor, S. et al. (2001). TBX1 is responsible for cardiovascular defects in velo-cardio-facial/DiGeorge syndrome. *Cell* **104**, 619-629.

Miller, C. T., Schilling, T. F., Lee, K., Parker, J. and Kimmel, C. B. (2000). sucker encodes a zebrafish Endothelin-1 required for ventral pharyngeal arch development. *Development* **127**, 3815-3828.

Moens, C. B. and Fritz, A. (1999). Techniques in neural development. *Methods Cell Biol.* **59**, 253-272.

Nikaido, M., Kawakami, A., Sawada, A., Furutani-Seiki, M., Takeda, H. and Araki, K. (2002). Tbx24, encoding a T-box protein, is mutated in the zebrafish somite-segmentation mutant fused somites. *Nat. Genet.* **31**, 195-199.

Peyrieras, N., Strahle, U. and Rosa, F. (1998). Conversion of zebrafish blastomeres to an endodermal fate by TGF-beta-related signaling. *Curr. Biol.* **8**, 783-786.

Piotrowski, T., Schilling, T. F., Brand, M., Jiang, Y. J., Heisenberg, C. P., Beuchle, D., Grandel, H., van Eeden, F. J., Furutani-Seiki, M., Granato, M. et al. (1996). Jaw and branchial arch mutants in zebrafish II: anterior arches and cartilage differentiation. *Development* **123**, 345-356.

Piotrowski, T. and Nüsslein-Volhard, C. (2000). The endoderm plays an important role in patterning the segmented pharyngeal region in zebrafish (Danio rerio). *Dev. Biol.* **225**, 339-356.

Rauch, G. J., Hammerschmidt, M., Blader, P., Schauerte, H. E., Strahle, U., Ingham, P. W., McMahon, A. P. and Haffter, P. (1997). Wnt5 is required for tail formation in the zebrafish embryo. *Cold Spring Harb. Symp. Quant. Biol.* **62**, 227-234.

Reifers, F., Bohli, H., Walsh, E. C., Crossley, P. H., Stainier, D. Y. and Brand, M. (1998). Fgf8 is mutated in zebrafish acerebellar (ace) mutants and is required for maintenance of midbrain-hindbrain boundary development and somitogenesis. *Development* **125**, 2381-2395.

Renucci, A., Lemarchandel, V. and Rosa, F. (1996). An activated form of type I serine/threonine kinase receptor TARAM-A reveals a specific signalling pathway involved in fish head organiser formation. *Development* **122**, 3735-3743.

Rubinstein, A. L., Lee, D., Luo, R., Henion, P. D. and Halpern, M. E. (2000). Genes dependent on zebrafish cyclops function identified by AFLP differential gene expression screen. *Genesis* **26**, 86-97.

Ryan, A. K., Goodship, J. A., Wilson, D. I., Philip, N., Levy, A., Seidel, H., Schuffenhauer, S., Oechsler, H., Belohradsky, B., Prieur, M. et al. (1997). Spectrum of clinical features associated with interstitial chromosome 22q11 deletions: a European collaborative study. *J. Med. Genet.* **34**, 798-804.

Scambler, P. J. (2000). The 22q11 deletion syndromes. *Hum. Mol. Genet.* **9**, 2421-2426.

Schilling, T. F., Piotrowski, T., Grandel, H., Brand, M., Heisenberg, C. P., Jiang, Y. J., Beuchle, D., Hammerschmidt, M., Kane, D. A., Mullins, M. C. et al. (1996). Jaw and branchial arch mutants in zebrafish I: branchial arches. *Development* **123**, 329-344.

Schulte-Merker, S., van Eeden, F. J., Halpern, M. E., Kimmel, C. B. and Nüsslein-Volhard, C. (1994). no tail (ntl) is the zebrafish homologue of the mouse T (Brachyury) gene. *Development* **120**, 1009-1015.

Srivastava, D., Thomas, T., Lin, Q., Kirby, M. L., Brown, D. and Olson, E. N. (1997). Regulation of cardiac mesodermal and neural crest development by the bHLH transcription factor, dHAND. *Nat. Genet.* **16**, 154-160.

Stalmans, I., Lambrechts, D., de Smet, F., Jansen, S., Wang, J., Maity, S., Kneer, P., von Der Ohe, M., Swillen, A., Maes, C. et al. (2003). VEGF: a modifier of the del22q11 (DiGeorge) syndrome? *Nat. Med.* **9**, 173-182.

Thomas, T., Kurihara, H., Yamagishi, H., Kurihara, Y., Yazaki, Y., Olson, E. N. and Srivastava, D. (1998). A signaling cascade involving endothelin-1, dHAND and msx1 regulates development of neural-crest-derived branchial arch mesenchyme. *Development* **125**, 3005-3014.

Trumpp, A., Depew, M. J., Rubenstein, J. L., Bishop, J. M. and Martin, G. R. (1999). Cre-mediated gene inactivation demonstrates that FGF8 is required for cell survival and patterning of the first branchial arch. *Genes Dev.* **13**, 3136-3148.

Tucker, A. S., Yamada, G., Grigoriou, M., Pachnis, V. and Sharpe, P. T. (1999). Fgf-8 determines rostral-caudal polarity in the first branchial arch. *Development* **126**, 51-61.

Vitelli, F., Taddei, I., Morishima, M., Meyers, E. N., Lindsay, E. A. and Baldini, A. (2002). A genetic link between Tbx1 and fibroblast growth factor signaling. *Development* **129**, 4605-4611.

Weinberg, E. S., Allende, M. L., Kelly, C. S., Abdelhamid, A., Murakami, T., Andermann, P., Doerre, O. G., Grunwald, D. J. and Riggleman, B. (1996). Developmental regulation of zebrafish MyoD in wild-type, no tail and spadetail embryos. *Development* **122**, 271-280.

Weinstein, B. M., Stemple, D. L., Driever, W. and Fishman, M. C. (1995). Gridlock, a localized heritable vascular patterning defect in the zebrafish. *Nat. Med.* **1**, 1143-1147.

Whitfield, T. T., Granato, M., van Eeden, F. J., Schach, U., Brand, M., Furutani-Seiki, M., Haffter, P., Hammerschmidt, M., Heisenberg, C. P., Jiang, Y. J. et al. (1996). Mutations affecting development of the zebrafish inner ear and lateral line. *Development* **123**, 241-254.

Yamagishi, H., Maeda, J., Hu, T., McAnally, J., Conway, S. J., Kume, T., Meyers, E. N., Yamagishi, C. and Srivastava, D. (2003). Tbx1 is regulated by tissue-specific forkhead proteins through a common Sonic hedgehog-responsive enhancer. *Genes Dev.* **17**, 269-281.